Article

Energy and Electron Transfer in Bifunctional Non-Conjugated Dendrimers

K. R. Justin Thomas, Alexis L. Thompson, Aathimanikandan
V. Sivakumar, Christopher J. Bardeen, and S. Thayumanavan

J. Am. Chem. Soc., **2005**, 127 (1), 373-383• DOI: 10.1021/ja044778m • Publication Date (Web): 16 December 2004

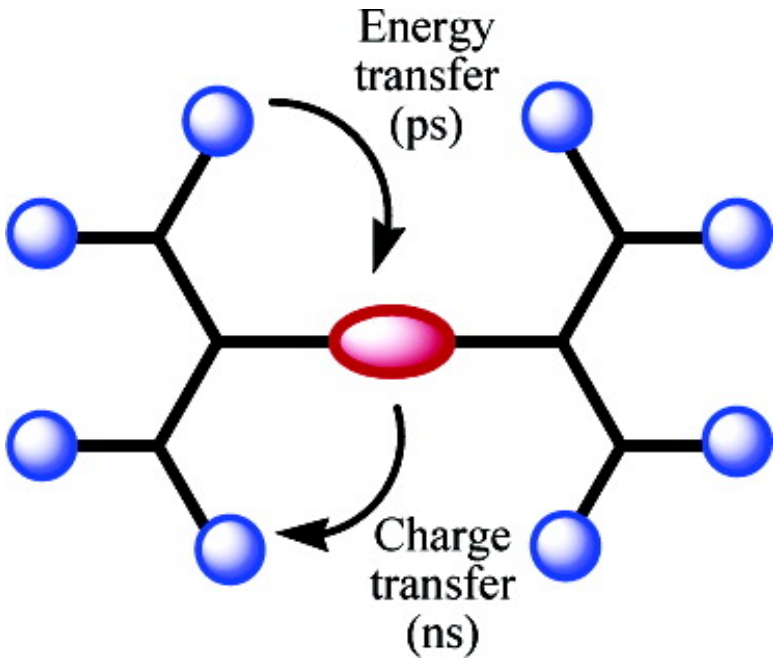

More About This Article

Additional resources and features associated with this article are available within the HTML version:

- Supporting Information
- Links to the 22 articles that cite this article, as of the time of this article download
- Access to high resolution figures
- Links to articles and content related to this article
- Copyright permission to reproduce figures and/or text from this article

View the Full Text HTML

J|A|C|S
ARTICLES
Published on Web 12/16/2004

Energy and Electron Transfer in Bifunctional Non-Conjugated Dendrimers

K. R. Justin Thomas,[†] Alexis L. Thompson,[‡] Aathimanikandan V. Sivakumar,[†] Christopher J. Bardeen,*[,‡] and S. Thayumanavan*[,†]

Contribution from the Department of Chemistry, University of Massachusetts, Amherst, Massachusetts 01003 and Department of Chemistry, University of Illinois, Urbana, Illinois 61801

Received August 30, 2004; E-mail: bardeen@scs.uiuc.edu; thai@chem.umass.edu

Abstract: Nonconjugated dendrimers, which are capable of funneling energy from the periphery to the core followed by a charge-transfer process from the core to the periphery, have been synthesized. The energy and electron donors involve a diarylaminopyrene unit and are incorporated at the periphery of these dendrimers. The energy and electron acceptor is at the core of the dendrimer, which involves a chromophore based on a benzthiadiazole moiety. The backbone of the dendrimers is benzyl ether based. A direct electron-transfer quenching of the excited state of the periphery or a sequential energy transfer−electron-transfer pathway are the two limiting mechanisms of the observed photophysical properties. We find that the latter mechanism is prevalent in these dendrimers. The energy transfer occurs on a picosecond time scale, while the charge-transfer process occurs on a nanosecond time scale. The lifetime of the charge separated species was found to be in the range of microseconds. Energy transfer efficiencies ranging from 80% to 90% were determined using both steady-state and time-resolved measurements, while charge-transfer efficiencies ranging from 70% to 80% were deduced from fluorescence quenching of the core chromophore. The dependence of the energy and charge-transfer processes on dendrimer generation is analyzed in terms of the backfolding of the flexible benzyl ether backbone, which leads to a weaker dependence of the energy and charge-transfer efficiencies on dendrimer size than would be expected for a rigid system.

Introduction

Designing efficient light harvesting materials is an important goal, considering the need for effectively using renewable energy sources.[1] Nature has already evolved an effective pathway for harvesting sunlight in to useful chemical energy that is stored in the form of ATP. Nature's light harvesting assembly, as exemplified in purple photosynthetic bacteria, consists of a multichromophore array that is capable of absorbing photons of a broad spectral range from the sunlight.[2] The placement of the chromophores relative to the reaction center plays a crucial role in the high efficiency of this light harvesting process.[3] The photosynthetic apparatus involves two key steps: (*i*) electronic energy transfer (EET) where the solar energy is funneled to a reaction center and (*ii*) a sequence of charge transfer (CT) events from the excited state of the reaction center that ultimately results in chemical energy. While the nature's light harvesting systems are extremely efficient in their native conditions, these systems are neither cheap nor robust enough to be widely useful as components of solar cells. Considering this, several groups have been interested in developing light harvesting systems with custom-designed molecules.[4] These molecules include small covalent arrays containing photoactive units,[5] or supramolecular,[6] and polymeric[7] systems containing multichromophore arrays.

Dendrimers,[8] which consist of peripheral units, a core, and intervening branching units, are interesting scaffolds for light harvesting applications. The decreasing number of functionalities from the periphery to the core of the dendrimer makes these molecules excellent candidates for light harvesting antenna (Figure 1). The periphery of the dendrimers functionalized with light absorbing chromophores could funnel the energy to a lower energy acceptor at the core. Since dendrimers are assembled layer-by-layer and can be synthesized with excellent control in molecular weight, control over the relative placement of photoactive units can be easily achieved.[8,9] Considering this possibility, several groups have utilized dendrimers as light

[†] Department of Chemistry, University of Massachusetts.
[‡] Department of Chemistry, University of Illinois.

(1) Hoffert, M. I.; Caldeira, K.; Jain, A. K.; Haites, E. K.; Harvey, L. D. D.; Potter, S. D.; Schlessinger, M. E.; Schnedier, S. H.; Watts, R. G.; Wigley, T. M.; Wuebbles, D. J. *Nature* **1998**, *395*, 881.
(2) (a) McDermott, G.; Prince, S. M.; Freer, A. A.; Hawthornthwaite-Lawless, A. M.; Papiz, M. Z.; Cogdell, R. J.; Isaacs, N. W. *Nature* **1995**, *374*, 517. (b) Pullerits, T.; Sundström, V. *Acc. Chem. Res.* **1996**, *29*, 381. (c) Kühlbrandt, W.; Wang, D. N.; Fujiyoshi, Y. *Nature* **1994**, *367*, 614.
(3) (a) Hu, Y. Z.; Takashima, H.; Tsukiji, S.; Shinkai, S.; Nagamune, T.; Oishi, S.; Hamachi, I. *Chem. Eur. J.* **2000**, *6*, 1907. (b) Hu, X.; Damjanovic, A.; Ritz, T.; Schulten, K. *Proc. Nat. Acad. Sci. U.S.A.* **1998**, *95*, 5935. (c) Oijen, A. M. V.; Ketelaars, M.; Köhler, J.; Aartsma, T. J.; Schmidt, J. *Science* **1999**, *285*, 400.
(4) (a) Gust, D.; Moore, T. A.; Moore, A. L. *Acc. Chem. Res.* **2001**, *34*, 40. (b) Wasielewski, M. R. *Chem. Rev.* **1992**, *92*, 435. (c) Fox, M. A. *Acc. Chem. Res.* **1999**, *32*, 201. (d) Balzani, V. *Tetrahedron* **1992**, *48*, 10443. (e) Wagner, R. W.; Johnson, T. E.; Lindsey, J. S. *J. Am. Chem. Soc.* **1996**, *118*, 11166. (f) Kurreck, H.; Huber, M. *Angew. Chem., Int. Ed. Engl.* **1995**, *34*, 849. (g) Hagfeldt, A.; Grätzel, M. *Acc. Chem. Res.* **2000**, *33*, 269. (h) Choi, M.-S.; Yamazaki, T.; Yamazaki, I.; Aida, T. *Angew. Chem., Int. Ed.* **2004**, *43*, 150.

10.1021/ja044778m CCC: $30.25

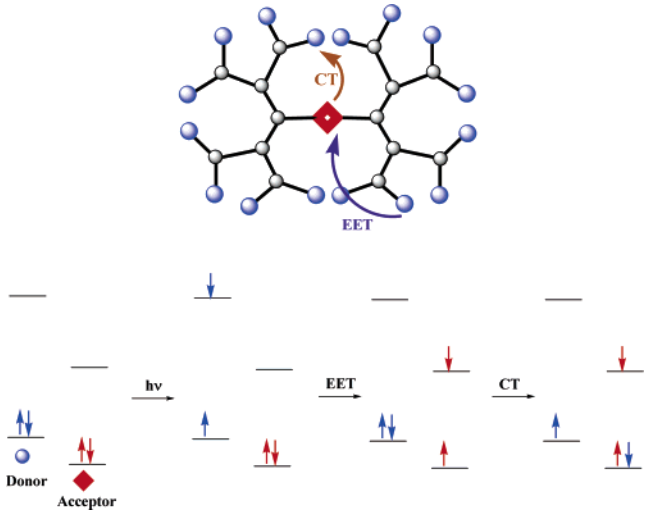

Figure 1. Cartoon of dendrimers for light harvesting.

harvesting antennae, in which efficient energy transfer from the periphery to the core of the dendrimer has been observed.[10] Studies have been carried out both with conjugated[11] and nonconjugated[12] dendrimers.

There has also been considerable effort to design dendrimers with favorable electron-transfer properties.[13] Efforts to combine these two steps, energy transfer and charge transfer, to mimic both preliminary events of the photosynthetic apparatus, have been more limited.[14] This sequence of events is outlined in Figure 1, where a donor molecule first transfers its energy to the core acceptor, which then is able to oxidize the donor and form a charge separated state. In such a system, the donor fulfills two roles: energy harvester and electron donor. It is easy to imagine that dendrimers are also interesting scaffolds for photoinduced charge transfer from the core to the periphery. As one moves from the core to the periphery of the dendrimers, the number of units at least doubles with each layer. Therefore, dendrimers could provide an entropic driving force for charge separation from the core to the periphery. Guldi et al. reported conjugated phenylene vinylene based dendrimers, in which an energy level dependent energy transfer and/or electron transfer was achieved.[14a] Qu et al. reported polypheneylene based conjugated, rigid dendrimers in which intramolecular energy transfer and electron transfer were observed.[14b] In this paper, we report on a nonconjugated dendrimer, in which energy transfer from the periphery to the core of the dendrimer is followed by an electron-transfer quenching of the core excited state. In conjugated dendrimers, the backbone serves as a vehicle for the through-bond communication both for electron and energy transfer. However, in nonconjugated dendrimers, the role

(5) (a) Sazanovich, I. V.; Kiramaier, C.; Hindin, E.; Yu, L.; Bocian, D. F.; Lindsey, J. S.; Holten, D. *J. Am. Chem. Soc.* **2004**, *126*, 2664. (b) Tomizaki, K.-y.; Yu, L.; Wei, L.; Bocian, D. F.; Lindsey, J. S. *J. Org. Chem.* **2003**, *68*, 8199. (c) Campagna, S.; Serroni, S.; Puntoriero, F.; Loiseau, F.; De Cola, L.; Kleverlaan, C. J.; Becher, J.; Sorensen, A. P.; Hascoat, P.; Thorup, N. *Chem. Eur. J.* **2002**, *8*, 4461. (d) Jullien, L.; Canceill, J.; Valeur, B.; Bardez, E.; Lefèvre, J.-P.; Lehn, J.-M.; Marchi-Artzner, V.; Pansu, R. *J. Am. Chem. Soc.* **1996**, *118*, 5432. (e) Liddell, P. A.; Kodis, G.; Andreasson, J.; De la Garza, L.; Bandyopadhyay, S.; Mitchell, R. H.; Moore, T. A.; Moore, A. L.; Gust, D. *J. Am. Chem. Soc.* **2004**, *126*, 4803. (f) Kodis, G.; Herrero, C.; Palacios, R.; Marno-Ochoa, E.; Gould, S.; De la Garza, L.; Van Grondelle, R.; Gust, D.; Moore, T. A. Moore, A. L. *J. Phys. Chem. B.* **2004**, *108*, 414. (g) Bennett, I. M.; Farfano, H. M. V.; Bogan, F.; Primak, A.; Liddell, P. A.; Otero, L.; Sereno, L.; Juana, J.; Moore, A. L.; Moore, T. A.; Gust, D. *Nature* **2002**, *420*, 398. (h) Weiss, E. A.; Chemick, E. T.; Wasielewski, M. R. *J. Am. Chem. Soc.* **2004**, *126*, 2326. (i) Gaimo, J. M.; Gusev, A. V.; Wasielewski, M. R. *J. Am. Chem. Soc.* **2002**, *124*, 8530. (j) Bell, T. D. M.; Ghiggino, K. P.; Jolliffe, K. A.; Ranasinghe, M. G.; Langford, S. J.; Shephard, M. J.; Paddon-Row: M. N. *J. Phys. Chem. A.* **2002**, *106*, 10079. (k) Biemans, H. A. M.; Rowan, A. E.; Verhoeven, A.; Vanoppen, P.; Latterini, L.; Foekema, J.; Schenning, A. P. H. J.; Meijer, E. W.; de Schryver, F. C.; Nolte, R. J. M. *J. Am. Chem. Soc.* **1998**, *120*, 11054.

(6) (a) Belser, P.; von Zelewsky, A.; Frank, M.; Seel, C.; Vögtle, F.; De Cola, L.; Barigelletti, F.; Balzani, V. *J. Am. Chem. Soc.* **1993**, *115*, 4076. (b) Balaban, T. S.; Goddard, R.; Linke-Schaetzel, M.; Lehn, J.-M. *J. Am. Chem. Soc.* **2003**, *125*, 4233. (c) Balaban, T. S.; Eichhofer, A.; Lehn, J.-M. *Chem. Eur. J.* **2000**, 6, 4047. (d) Kercher, M.; König, B.; Zieg, H.; De Cola, L. *J. Am. Chem. Soc.* **2002**, *124*, 11541. (e) Takahashi, R.; Kobuke, Y.; *J. Am. Chem. Soc.* **2003**, *125*, 2372. (f) Anderson, S.; Anderson, H. L.; Bashall, A.; McPartlin, M.; Sanders, J. K. M. *Angew. Chem., Int. Ed. Engl.* **1995**, *34*, 1096. (g) Drain, C. M.; Nifiatis, F.; Vasenko, A.; Batteas, J. D. *Angew. Chem., Int. Ed.* **1998**, *37*, 2344. (h) Prodi, A.; Indelli, M. T.; Kleverlaan, C. J.; Scandola, F.; Alessio, E.; Gianferrata, T.; Marzilli, L. G. *Chem. Eur. J.* **1999**, *5*, 2668. (i) Sugou, K.; Sasaki, K.; Iwaki, T.; Kuroda, Y. *J. Am. Chem. Soc.* **2002**, *124*, 1182.

(7) (a) Webber, S. E. *Chem. Rev.* **1990**, *90*, 1469. (b) Watkins, D. M.; Fox, M. A. *J. Am. Chem. Soc.* **1994**, *116*, 6441. (c) Fox, H. H.; Fox, M. A. *Macromolecules* **1995**, *28*, 4570. (d) Ng, D.; Guillet, J. E. *Macromolecules* **1982**, *15*, 724. (e) Ng, D.; Guillet, J. E. *Macromolecules* **1982**, *15*, 728. (f) Jones, G., II.; Rahman, M. A. *Chem. Phys. Lett.* **1992**, *200*, 241. (g) Sein, J.; Schultze, X.; Adronov, A.; Fréchet, J. M. J. *Macromolecules* **2002**, *35*, 5396. (h) Peng, K. Y.; Chen, S. A.; Fann, W. S. *J. Am. Chem. Soc.* **2001**, *123*, 11388.

(8) (a) Newkome, G. R.; Moorefield, C. N.; Vögtle, F. *Dendrimers and Dendrons: Concepts, Syntheses, Applications*, 2nd ed.; Wiley-VCH: New York, 2001. (b) *Dendrimers and Other Dendritic Polymers*; Fréchet, J. M. J., Tomlia, D. A., Eds.; John Wiley & Sons: New York, 2002. (c) Bosman, A. W.; Janssen, H. M.; Meijer, E. W. *Chem. Rev.* **1999**, *99*, 1665. (d) Fischer, M.; Vögtle, F. *Angew. Chem., Int. Ed. Engl.* **1999**, *38*, 884. (e) Fréchet, J. M. J. *Science* **1994**, *263*, 1710. (f) Matthews, O. A.; Shipway, A. N.; Stoddart, J. F. *Prog. Polym. Sci.* **1998**, *23*, 1. (g) *Dendrimers II: Architecture, Nanostructure and Supramolecular Chemistry*; Vögtle, F., Ed.; Springer: Berlin, 2000; Vol. 210. (h) Zeng, F.; Zimmerman, S. C. *Chem. Rev.* **1997**, *97*, 1681.

(9) For methodologies that allow variations among every monomer unit of a dendrimer, see: (a) Sivanandan, K.; Britto, S. S.; Thayumanavan, S. *J. Org. Chem.* **2004**, *69*, 2937. (b) Vutukuri, D.; Sivnandan, K.; Thayumanavan, S. *Chem. Commun.* **2003**, 796. (c) Sivanandan, K.; Vutukuri, D.; Thayumanavan, S. *Org. Lett.* **2002**, *4*, 3751.

(10) (a) Balzani, V.; Ceroni, P.; Maestri, M.; Vicinelli, V. *Curr. Opin. Chem. Biol.* **2003**, *7*, 657. (b) Adronov, A.; Fréchet, J. M. J. *Chem. Commun.* **2000**, 1701. (c) Balzani, V.; Campagna, S.; Denti, G.; Juris, A.; Serroni, S.; Venturi, M. *Acc. Chem. Res.* **1998**, *31*, 26. (d) Dirksen, A.; De Cola, L. *C. R. Chimie* **2003**, *6*, 873. (e) Serroni, S.; Campagna, S.; Puntoriero, F.; Loiseau, F.; Ricevuto, V.; Passalacqua, R.; Galletta, M. *C. R. Chimie* **2003**, *6*, 883. (f) Reference 4h.

(11) (a) Devadoss, C.; Bharathi, P.; Moore, J. S. *J. Am. Chem. Soc.* **1996**, *118*, 9635. (b) Shortreed, M. R.; Swallen, S. F.; Shi, Z.-Y.; Tan, W.; Xu, Z.; Devadoss, C.; Moore, J. S.; Kopelman, R. *J. Phys. Chem. B.* **1997**, *101*, 6318. (c) Mellinger, J. S.; Pan, Y.; Kleiman, V. D.; Peng, Z.; Davis, B. L.; McMorrow, D.; Lu, M. *J. Am. Chem. Soc.* **2002**, *124*, 12002. (d) Wang. Y.; Ranasinghe, M. I.; Goodson, T., III. *J. Am. Chem. Soc.* **2003**, *125*, 9562. (e) Ranasinghe, M. I.; Varnavski, O. P.; Pawlas, J.; Hauck, S. I.; Louie, J.; Hartwig, J.; Goodson, T., III. *J. Am. Chem. Soc.* **2002**, *124*, 6520. (f) Gronheid, R.; Hofkens, J.; Köhn, F.; Weil, T.; Reuther, E.; Müllen, K.; DeSchryver, F. C. *J. Am. Chem. Soc.* **2002**, *124*, 2418. (g) Weil, T.; Reuther, E.; Beer, C.; Müllen, K. *Chem. Eur. J.* **2004**, *10*, 1398. (h) Liu, D. J.; De Feyter, S.; Cotlet, M.; Stefan, A.; Wiesler, U. M.; Herrmann, A.; Grebel-Koehler, D.; Qu, J. Q.; Mullen, K.; De Schryver, F. C. *Macromolecules* **2003**, *36*, 5918. (i) Benites, M.d. R.; Johnson, T. E.; Weghorn, S.; Yu, L.; Rao, P. D.; Diers, J. R.; Yang, S. I.; Kirmaier, C.; Bocian, D. F.; Holten, D.; Lindsey, J. S. *J. Mater. Chem.* **2002**, *12*, 65.

(12) (a) Stewart, G. M.; Fox, M. A. *J. Am. Chem. Soc.* **1996**, *118*, 4354. (b) Jiang, D. L.; Aida, T. *J. Am. Chem. Soc.* **1998**, *120*, 10895. (c) Adronov, A.; Gilat, S. L.; Fréchet, J. M. J.; Ohta, K.; Neuwahl, F. V. R.; Fleming, G. R. *J. Am. Chem. Soc.* **2000**, *122*, 1175. (d) Neuwahl, F. V. R.; Righini, R.; Adronov, A.; Malenfant, P. R. L.; Fréchet, J. M. J. *J. Phys. Chem. B* **2001**, *105*, 1307. (e) Hahn, U.; Gorka, M.; Vögtle, F.; Vicinelli, V.; Ceroni, P.; Maestri, M.; Balzani, V. *Angew. Chem., Int. Ed.* **2002**, *41*, 3595. (f) Choi, M.-S.; Aida, T.; Yamazaki, T.; Yamazki, I. *Chem. Eur. J.* **2002**, *8*, 2668.

(13) (a) Lor, M.; Thielemans, J.; Viaene, L.; Cotlet, M.; Hofkens, J.; Weil, T.; Hampel, C. Mullen, K.; Verhoeven, J. W.; Van der Auweraer, M.; De Schryver, F. C. *J. Am. Chem. Soc.* **2002**, *124*, 9918. (b) Capitosti, G. J.; Cramer, S. J.; Rajesh, C. S.; Modarelli, D. A. *Org. Lett.* **2001**, *3*, 1645. (c) Sadamoto, R.; Tomioka, N.; Aida, T. *J. Am. Chem. Soc.* **1996**, *118*, 3978.

(14) (a) Guldi, D. M.; Swartz, A.; Luo, C.; Gómez, R.; Segura, J.; Martín, N. *J. Am. Chem. Soc.***2002**, *124*, 10875. (b) Qu, J.; Pschirer, N. G.; Liu, D.; Stefan, A.; De Schryver, F. C.; Müllen, K. *Chem. Eur. J.* **2004**, *10*, 528. (c) For a study in which the branching units are partially oxidized to generate a mixed valence compound, which was involved in an electron-transfer quenching of the excited state of light absorber, see: Belser, P.; von Zelewsky, A.; Frank, M.; Seel, M. Vögtle, F.; De Cola, L.; Bargelletti, F.; Balzani, V. *J. Am. Chem. Soc.* **1993**, *115*, 4076. (d) Choi, M.-S.; Aida, T.; Luo, H.; Araki, Y.; Ito, O. *Angew. Chem., Int. Ed.* **2003**, *42*, 4060.

Chart 1. Structures of Dendrimers and Model Compounds

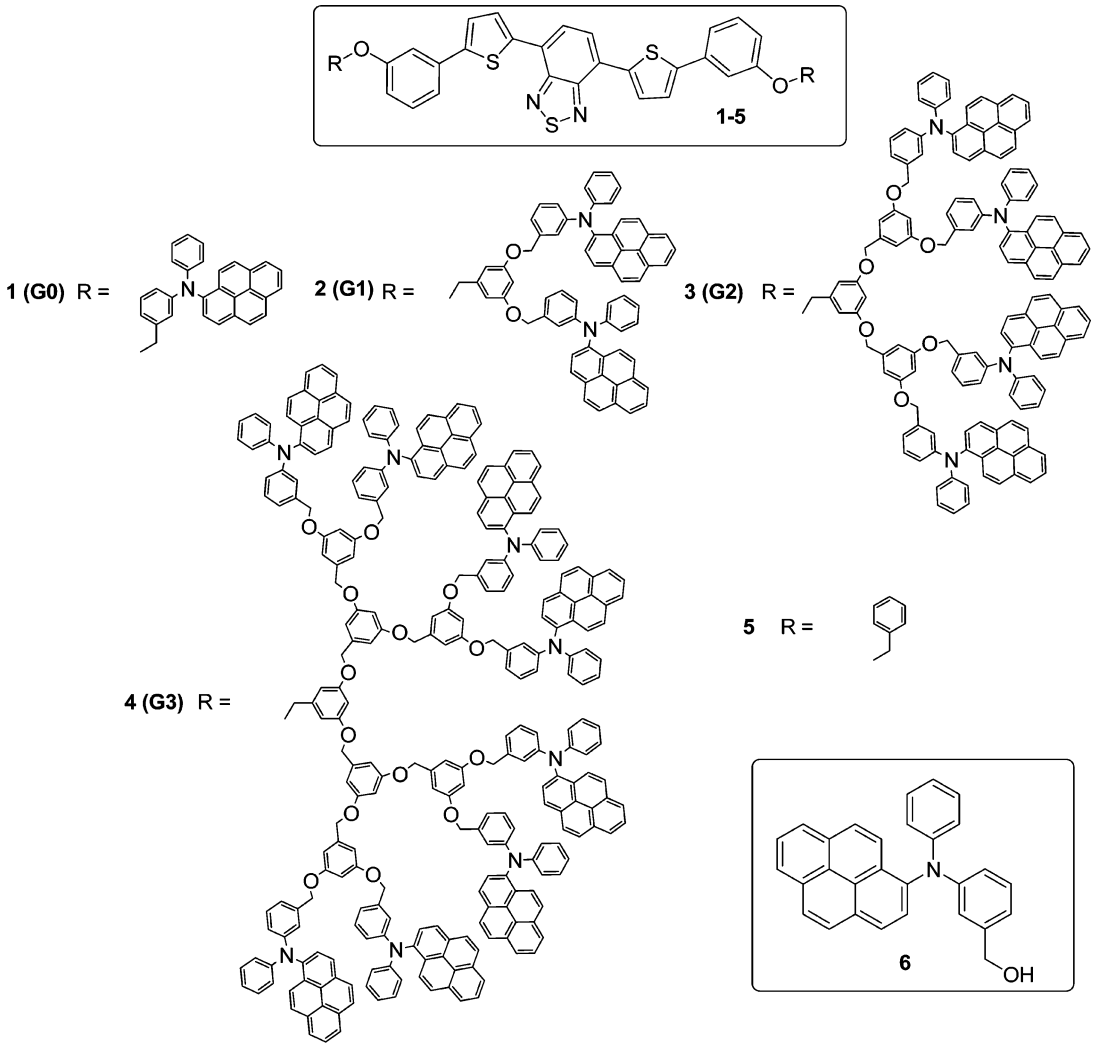

of the backbone is only structural and not functional. Therefore, studying these dendrimers should be useful in dissecting the architectural advantages of dendrimers as light harvesting materials. In addition, a nonconjugated backbone also provides the ability to independently tune the energy levels of the donors and acceptors. The flexibility of the dendrimer arms may enhance solubility, and also provide a way for the molecule to compact itself via folding. Our molecular system consists of benzyl ether dendrons functionalized with diarylaminopyrene units in the periphery attached to benzthiadiazole core. We find that this series of dendrimers exhibits picosecond energy transfer from the periphery to the core followed by nanosecond charge transfer from the core to the periphery. The lifetime of the charge separated state was found to be in the microsecond time scale. Furthermore, we find that while the EET rate decreases with dendrimer branch length, the CT rate (as deduced from fluorescence quenching of the core) remains essentially unchanged.

Results and Discussion

Synthesis and Characterization. Structures of the dendrimers, control core chromophore **5**, and the control peripheral diarylaminopyrene **6** are shown in Chart 1. The dendrimers contain diarylaminopyrene moieties as the energy donor at the periphery, 3,5-dihydroxybenzyl alcohol as the nonconjugated repeat unit, and the benzthiadiazole-based chromophore unit as the core. Syntheses of these dendrimers were approached in a modular fashion using the convergent approach. Thus, the benzthiadiazole based core chromophore containing two phenolic functionalities and the diarylaminopyrene containing dendrons were synthesized separately and then assembled in the last step (vide infra). Synthesis of the chromophore core **9** was achieved using a two-step one-pot procedure starting form 4,7-bis(5-bromothiophen-2-yl)benz[*c*][1,2,5]thiadiazole (**7**) and the aryl stannane **8**. These two compounds were coupled using the Stille methodology,[15] with $Pd(PPh_3)_2Cl_2$ as the catalyst and DMF as the solvent. This reaction was followed by a desilylation procedure with aqueous KF in the same pot (Scheme 1). Note that aqueous KF is commonly used as a reagent to wash-off the tin-based byproducts in the Stille coupling reactions. In our case, this solution also served to cleave the *tert*-butyldimethylsilyl protecting groups.

Synthesis of the peripheral unit **6** was achieved using the palladium catalyzed C−N coupling reaction as the key step (Scheme 2). To synthesize the aldehyde intermediate **13**, we attempted the reaction between *N*-phenyl-1-pyrenylamine (**10**)

(15) Stille, J. K. *Angew. Chem., Int. Ed. Engl*. **1986**, *25*, 508.

Scheme 1

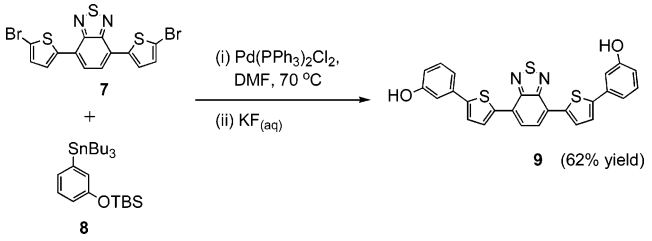

Scheme 2

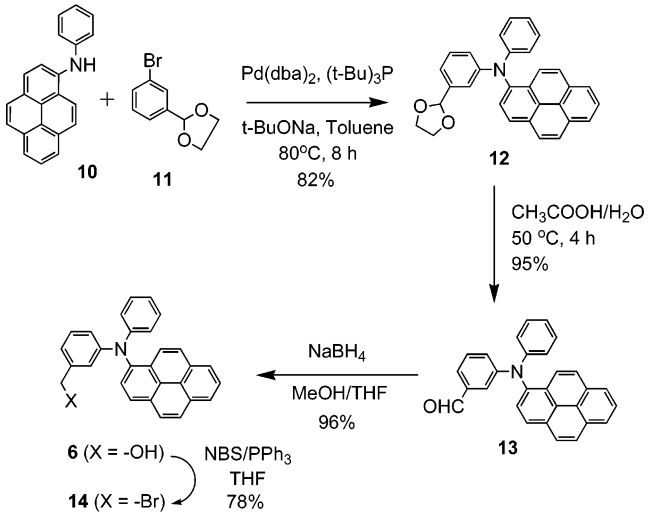

and 3-bromobenzaldehyde under Hartwig's conditions ($Pd(dba)_2$, $P(t\text{-}Bu)_3$, *t*-BuONa, Toluene, 80 °C).[16] The reaction failed to afford any desired compound. Using less active bases such as K_2CO_3 or Cs_2CO_3 produced only trace amounts of product. When the reaction was carried out with the protected derivative, 2-(3-bromophenyl)-1,3-dioxolane (**11**), the product **12** was obtained in 82% yield. Deprotection of the acetal moiety by treatment with acetic acid resulted in the aldehyde **13** in 95% yield. The aldehyde moiety was then reduced to the corresponding hydroxymethyl group to afford the peripheral triarylamine **6**. This compound was used as the model for the energy donor component of the dendrimers **1**−**4**. The hydroxymethyl group was then converted to the corresponding bromomethyl compound **14** upon treatment with NBS/PPh_3. Compound **14** was used for further elaboration in to the dendrons.

In the convergent assembly of dendrons, compound **14** was treated with 3,5-dihydroxybenzyl alcohol **(15)** under Williamson alkylation conditions to afford the G-1 dendron **16** in 78% yield (Scheme 3). Conversion of the hydroxymethyl compound **16** to the bromomethyl version **17** was achieved using NBS/PPh_3. Note that the success of this second step depends on the use of concentrated mixture and short reaction time. Compound **17** was taken through the above two synthetic steps iteratively to obtain the G-2 and G-3 monodendrons **19** and **21** with a bromomethyl functionality at the focal point. In the final step of the assembly, the bromomethyl functionalized compounds **14** (G0), **17**(G1), **19** (G2), and **21** (G3) were treated with the phenol functionalized core **9** in the similar fashion using K_2CO_3 and 18-Crown-6 in THF to obtain the dendrimers **1**, **2**, **3**, and **4** respectively.

All new compounds were characterized by ^1H, ^{13}C NMR, and mass spectrometry. As successive generations were added, multiple NMR signals attributable to the benzylic protons were observed. For instance, only one benzylic signal is observed for compounds **1** and **5**. However, four different signals in the ratio of 8:4:2:1 are observed in the case of **4**. All the dendrimers exhibited the parent ion peak with calculated isotopic distribution pattern in the MALDI-ToF spectra. Additionally, the purity of the samples was also elucidated using GPC. All dendrimers exhibited a single sharp peak in the size exclusion chromatogram indicating the presence of a single large species. We also characterized the dendrimers **1**−**4** using absorption spectra. The relative number of the diarylaminopyrene periphery units and the benzthiadiazole core increases with increasing generation. It is expected then that there will be a linear increase in the relative absorbance of these two species in dendrimers **1**−**4**. Our observations are consistent with these expectations (vide infra).

Steady-State Absorption and Emission Spectroscopy. We have used both linear absorption and emission spectroscopy for the photophysical characterization of the dendrimers. Absorption spectra of compounds **1**, **5**, and **6** are shown in Figure 2. The spectrum of compound **5** represents the absorption characteristics of the core chromophore, since this molecule does not contain any diarylaminopyrene donor. Similarly, the spectrum of compound **6** represents the absorption features of the diarylaminopyrene unit. The spectrum of compound **1** can be very well approximated by a weighted sum of the absorption spectra of compounds **5** and **6**. Similar behavior is also observed for the dendrimers **2**−**4**. This provides evidence for the lack of direct electronic communication between the diarylaminopyrene periphery and the benzthiadiazole core in the ground electronic state.

Comparison of the absorption spectra of the dendrons G0 through G3 (**1** through **4**) shows that the absorbance of these compounds increases steadily with increasing generation. This is attributed to the increasing number of diarylaminopyrene units with generation. We utilized this feature to further assert the identity of the chromophore-cored dendrimers **1**−**4**. Figure 3 shows that the absorbance at 395 nm increases steadily with generation when normalized for the chromophore core absorption at 490 nm. A plot of the number of pyrene units with the absorbance at 395 nm for compounds **1**−**5** exhibits a linear relationship that passes through the origin (see inset in Figure 3). This further attests to the purity of the dendrimers studied.

The emission spectrum of the control molecule **5** has the maxima centered at 602 nm, when excited at 490 nm. Similarly, excitation of the diarylaminopyrene molecule **6** at 395 nm exhibits an emission spectrum with the maxima centered at 464 nm. The emission maxima for the dendrimers **1**−**4** is fairly insensitive to the excitation wavelength, with most of the emission centered around 600 nm. Since this peak corresponds to the chromophore core, this is taken as preliminary evidence to suggest that there is an efficient energy transfer from the diarylaminopyrene unit to the chromophore core in all these dendrimers. The efficiency of the energy transfer process was quantified using both steady-state and time-resolved spectroscopic data (vide infra).

(16) (a) Hartwig, J. F. *Angew. Chem., Int. Ed. Engl.* **1998**, *37*, 2046. (b) Wolfe, J. P.; Wagaw, S.; Marcoux, J.-F.; Buchwald, S. L. *Acc. Chem. Res.* **1998**, *31*, 805. (c) For a C−N bond formation methodology that uses a cheaper copper based catalyst, see: Gujadhur, R. K.; Bates, C. G.; Venkataraman, D. *Org. Lett.* **2001**, *3*, 4315.

Scheme 3

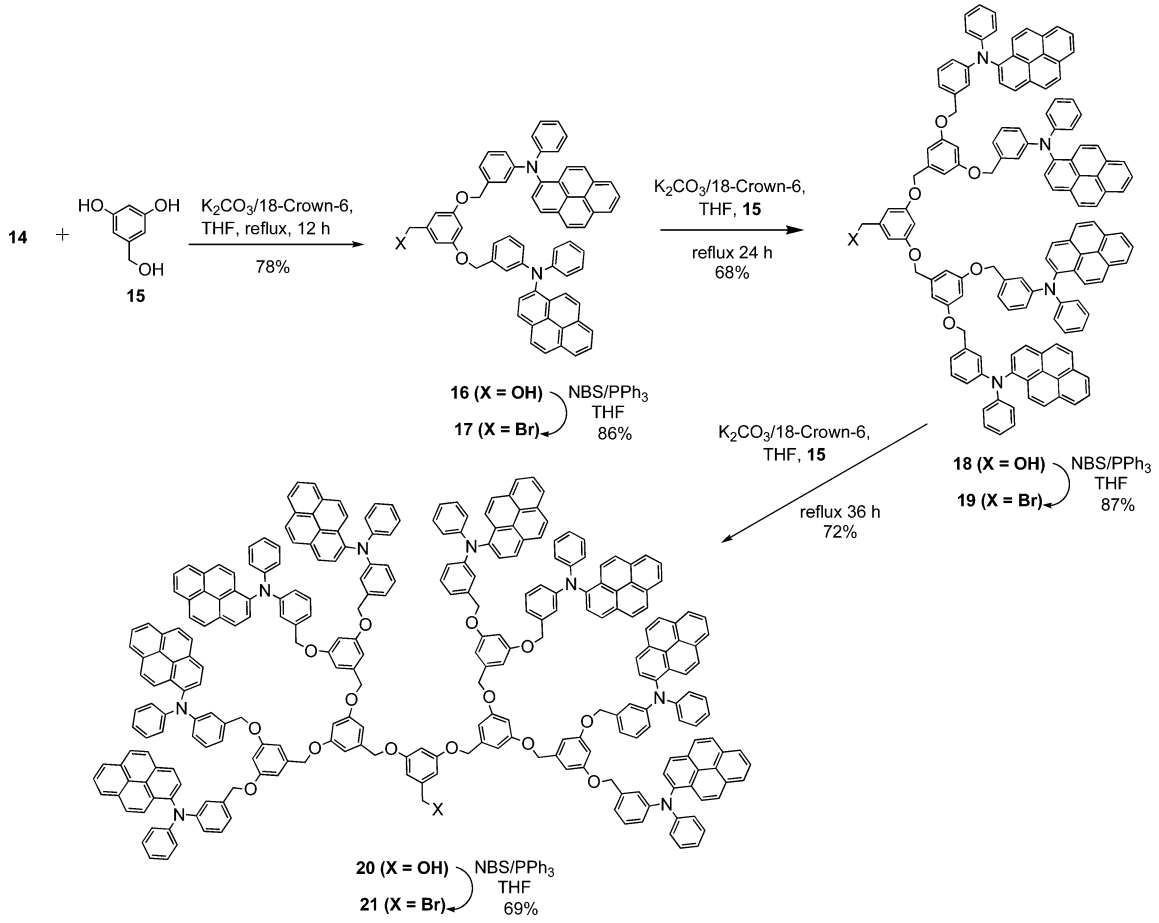

Energy Level Estimations. As mentioned above, we hypothesized that these dendrimers should be capable of sequentially funneling energy from the chromophores at the periphery to the chromophore at the core followed by a charge-transfer quenching of the excited core by the functionalities in the periphery. In order for these processes to occur, the core and peripheral functionalities should have appropriate relative energies. We estimated the HOMO and LUMO energy levels using the combination of absorption and emission spectra along with electrochemical studies. The intersection of the absorption and emission spectra was assumed to be an estimate of ΔE_{0-0} gap for the chromophores. Oxidation or reduction potential determined by electrochemistry were taken to be an estimate of the HOMO or LUMO of the molecule, respectively.

Cyclic voltammograms of the compounds **1** and **6** are shown in Figure 4. Redox potentials are reported with respect to ferrocene/ferrocenium couple as the internal standard. The

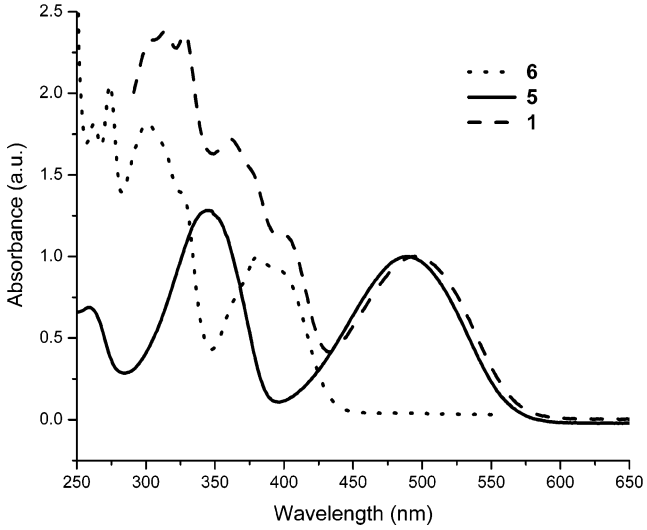

Figure 2. Absorption spectrum of compounds **1**, **5**, and **6**.

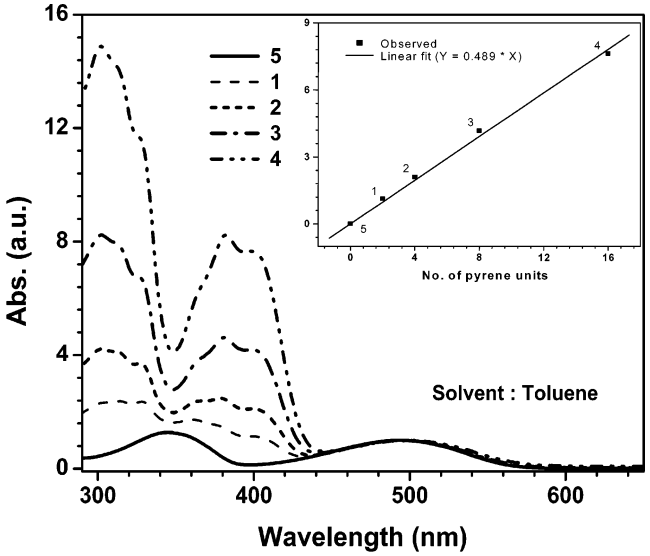

Figure 3. Comparison of absorption spectrum of compounds **1**−**5**. The spectrum is normalized at the low-energy peak that corresponds to the chromophore core. Inset: Plot of Number of pyrene in dendrimers vs absorbance at 395 nm.

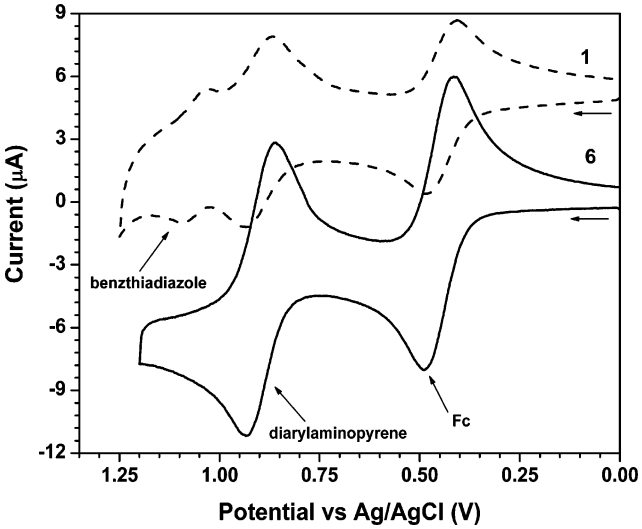

Figure 4. Cyclic voltammogram of compounds **1** and **6**.

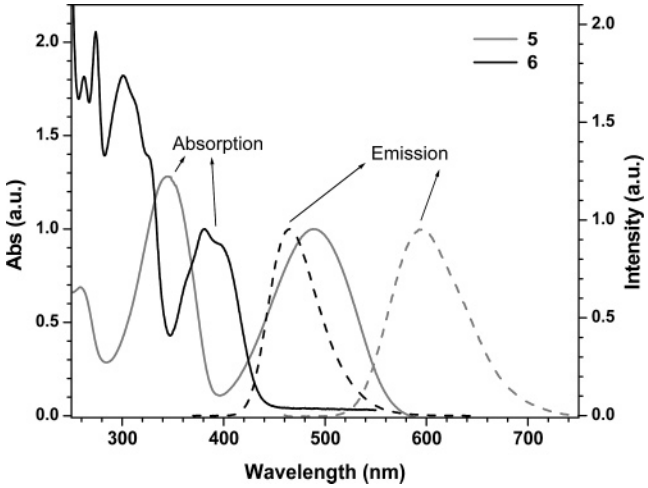

Figure 5. Absorption and emission spectra of compounds **5** and **6**. Note the overlap between the emission spectrum of **6** with the absorption spectrum of **5**.

benzthiadiazole core exhibited an oxidation potential of 595 mV and a reduction peak at −1674 mV. This corresponds to a HOMO−LUMO gap of about 2.27 eV. This value is close to the estimate of 2.18 eV that utilizes the ΔE_{0-0} calculated from the absorption and emission spectra. The oxidation potential of the diarylaminopyrene periphery **6** is centered at 444 mV. The ΔE_{0-0} for compound **6** was estimated to be 2.82 eV using the intersection of absorption and emission spectra. These estimates clearly suggest that the diarylaminopyrene functionality in the periphery of compounds **1**−**4** is capable of transferring energy to the benzthiadiazole core. It is also evident from these estimates that the excited state of the chromophore core could be reduced by the diarylaminopyrene moiety. As mentioned above, our dendrimer is designed to funnel the energy from the periphery to the core followed by a charge transfer process. Both these processes seem to be energetically feasible. It is to be noted however that it is also energetically feasible to obtain the final charge transfer product by directly quenching the excited state of the diarylaminopyrene periphery by electron transfer. To distinguish these possibilities, it is necessary to estimate the extent of energy transfer from the periphery to the core. This is addressed both using steady-state spectroscopy and time-resolved spectroscopy (see below). Time- and wavelength-resolved fluorescence measurements are obtained using a streak camera (Hamamatsu, streak scope C4334) attached to a spectrometer. The solutions are excited using 150 fs, 400 nm pulses, and the fluorescence is collected at 90° relative to the excitation beam. The emission is monitored from 420 to 750 nm, and no time dependence of the spectrum is observed. Additional information can be found in the Supporting Information.

Energy and Charge-Transfer Studies. Linear absorption and emission spectra of compounds **5** and **6** are shown in Figure 5. The overlap between the emission spectrum of **6** and the absorption spectrum of **5** indicates that Förster energy transfer is possible from diarylaminopyrene to the benzthiadiazole core. A calculation of the Förster radius for this donor−acceptor pair yields an R_0 of 48 Angstroms, which is quite large. Although excitation at 395 nm should excite mostly the diarylaminopyrene, the fluorescence of compounds **1**−**4** is dominated by emission from the benzthiadiazole core. Experiments on mixtures of **5** and **6** showed that intermolecular EET was nonexistent under our experimental conditions. To quantify the extent of energy transfer in compounds **1**−**4**, excitation spectra of these compounds were obtained at λ_{em} of the core at 603 nm. The excitation spectra were then compared with the respective absorption spectra. The relative ratio of the peaks corresponding to the donor, while normalizing for the peaks corresponding to the acceptor, was used to estimate the energy transfer efficiency.[17] The estimated quantum yields for energy transfer are 87%, 85%, 81%, and 79% for compounds **1**, **2**, **3**, and **4** respectively. These results show that energy transfer from the periphery to the core is the major pathway. This also shows that direct quenching of the excited state of the diarylaminopyrene by electron transfer is very small, if any. The fact that these energy transfer efficiencies are relatively insensitive to the polarity of solvents further supports the mechanism.

These high EET efficiencies are consistent with the picosecond time-resolved data shown in Figure 6 as well. In Figure 6a, we show the picosecond fluorescence decay for G0-G3, along with the results of a biexponential fit to the data. The fits consist of a fast component whose lifetime increases from 21 ps in G0 to 162 ps in G3, and a small, long-lived component with a lifetime which is obtained from the decay of **6**. Note that the long-lived component of the decay appears flat on the time scale of the figure. The results of our fits to the donor decays in DMF are summarized in Table 1. The short-time component is relatively insensitive to solvent, although it does decrease measurably in the two larger dendrimers, G2 and G3, by ∼34% in toluene and ∼18% in CH_2Cl_2 relative to the times obtained in DMF. In Figure 6b, we also show the short-time dynamics of the acceptor emission at 600 nm. As expected in a light-harvesting system, the acceptor exhibits a fast rise on a time scale similar to the donor decay.

The origin of the small long-lived component, whose lifetime is similar to that of the isolated donor, is an open question. Such a long-lived component of the donor population has been observed previously in other light-harvesting benzyl-ether dendrimers and ascribed to an energy transfer saturation phenomenon.[12d] The suggestion in those femtosecond pump−

(17) Haugland, R. P.; Yguerabide, J.; Stryer, L. *Proc. Natl. Acad. Sci. U.S.A.* **1969**, *63*, 23.

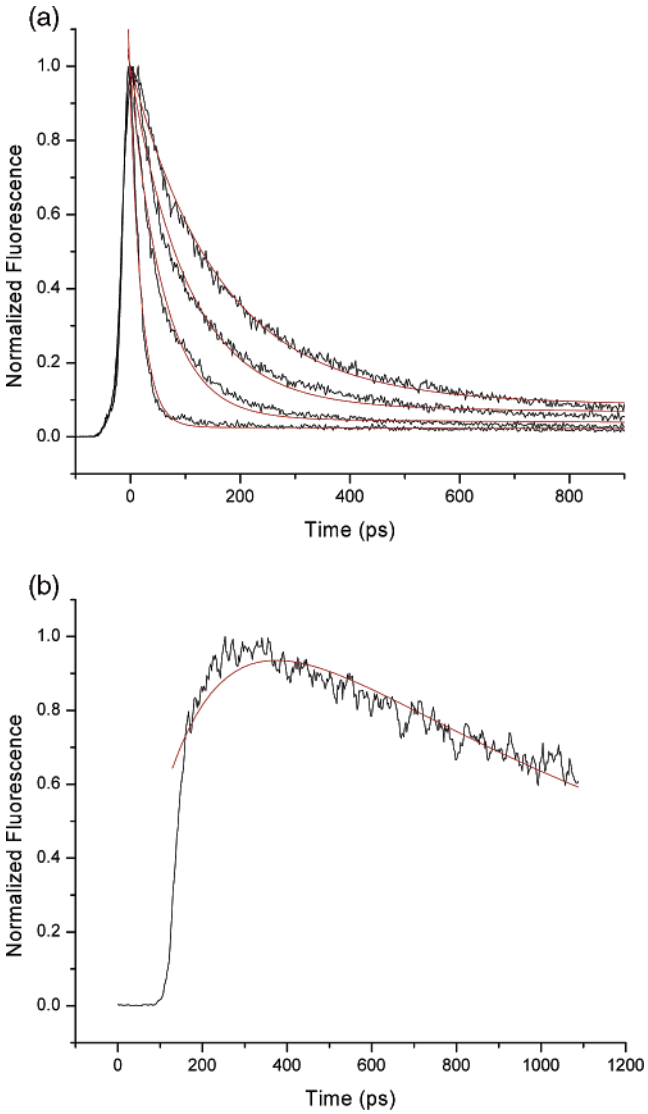

Figure 6. **a.** Picosecond donor fluorescence decays for G0 (**1**) (shortest decay), G1 (**2**), G2 (**3**), and G3 (**4**) (longest decay) in DMF. Biexponential fit lines for each molecule are shown in red. One time constant is fixed to the value fit from a longtime decay of the donor **6** fluorescence. Values are in Table 1. Figure 6b. Acceptor fluorescence signal for G3 (**4**) in DMF with triexponential fit (red) as discussed in the text. In the fitting, the decay times are fixed to the values for the long time acceptor decay (Table 3) and the short time donor decay Table 1, with the amplitudes allowed to vary.

Table 1. Fit Parameters for Curves Shown in Figure 6a[a]

	A_1	τ_1 (ps)	A_2	τ_2 (ns)
G0	0.889	21.2	0.025	9.88
G1	0.927	61.3	0.045	9.88
G2	0.911	104.8	0.077	9.88
G3	0.902	162.2	0.097	9.88

[a] The τ_2 times, which are obtained from the decay of **6**, are not allowed to vary in the fitting.

probe experiments was that high power excitation could excite two donors within a single dendrimer, only one of which could undergo energy transfer. The other donor would then remain in its excited state for the duration of its normal excited state lifetime. If this were the case, then one would expect a strong dependence of the slow decay component on the laser pulse energy, since the probability of having two excitations simultaneously on a single dendrimer should be roughly proportional to the square of the light intensity. The relative amplitudes of the fast and slow decay components were observed to be independent of laser power over 2 orders of magnitude, however, which effectively rules out this mechanism for the long decay. Another possible explanation is that the long-lived component results from residual donor impurities in our sample. Repeated purifications of the final product failed to change its amplitude appreciably, however. Aggregation of the chromophores might also be expected to lead to a separate, long-lived emission due to excimer formation. Generally, excimers have a broadened, redshifted emission with a longer lifetime due to a reduced radiative rate. This explanation is contradicted by two observations: that the spectrum of the long-lived species is identical to that of the short-lived species, i.e., the monomeric pyrene emission; and its lifetime is equal to or less than that of the monomer, instead of being longer. A final explanation is that conformational disorder in the dendrimers leads to a subpopulation where at least one donor is oriented such that its Forster transfer probability to the core is essentially zero. Such disorder would be expected to increase for the larger dendrimers, consistent with the increase in the amplitude of the long-lived component seen in Table 1. Nevertheless, we cannot rule out the possibility of impurity emission as well, and so we do not attempt to analyze the amplitude of the long-lived decay in any detail. Since in all cases it contributes 10% or less of the total signal, its role in the overall photophysics of these molecules is relatively minor.

To quantitatively describe the dendrimer photophysics, we use a simple kinetic model to describe the EET dynamics. First, to describe the donor dynamics, we must assume two separate populations of excited donors, $N^{(1)}_{\text{donor}}$ and $N^{(2)}_{\text{donor}}$, whose temporal evolution is described by the equations below

$$\frac{dN^{(1)}_{\text{donor}}}{dt} = -(k_{\text{EET}} + k_{\text{donor}})N^{(1)}_{\text{donor}} \quad (1)$$

$$\frac{dN^{(2)}_{\text{donor}}}{dt} = k_{\text{donor}}N^{(2)}_{\text{donor}} \quad (2)$$

$$\frac{dN_{\text{acc}}}{dt} = -k_{\text{acc}}N_{\text{acc}} + k_{\text{EET}}N^{(1)}_{\text{donor}} \quad (3)$$

where $N^{(1)}_{\text{donor}}$ represents the donor population that undergoes EET to the core, while the population $N^{(2)}_{\text{donor}}$ only undergoes its intrinsic fluorescence decay given by k_{donor}. Since the donor and acceptor emissions are well separated in these compounds, the two populations can be monitored independently. The observed fluorescence signals of both the donor and acceptor are then given by the biexponential functions

$$F_{\text{donor}}(t) = N^{(1)}_{\text{donor}}(0)\exp[-(k_{\text{EET}} + k_{\text{donor}})t] + N^{(2)}_{\text{donor}}(0)\exp[-k_{\text{donor}}t] \quad (4)$$

$$F_{\text{acc}}(t) = \left(\frac{k_{\text{EET}}N^{(1)}_{\text{donor}}(0)}{k_{\text{acc}} - k_{\text{EET}} - k_{\text{donor}}}\right)\exp[-(k_{\text{EET}} + k_{\text{donor}})t] + \left(N_{\text{acc}}(0) - \frac{k_{\text{EET}}N^{(1)}_{\text{donor}}(0)}{k_{\text{acc}} - k_{\text{EET}} - k_{\text{donor}}}\right)\exp[-k_{\text{acc}}t] \quad (5)$$

$N^{(1)}_{donor}(0)$, $N^{(2)}_{donor}(0)$ and $N_{acc}(0)$ are the initial excited-state populations created by the laser pulse, which are determined by the relevant concentrations and absorption coefficients. Equation 4 describes the observed biexponential decay of the donor, while eq 5 predicts that the acceptor signal also has two components: a rapid rise due to EET from the $N^{(1)}_{donor}$ population followed by a slower decay given by k_{acc}. While the relative sizes of $N^{(1)}_{donor}(0)$ and $N^{(2)}_{donor}(0)$ can be obtained directly from fitting the donor decay, the relative amplitudes of the prefactors in eq 5 can be obtained from the measured fluorescence decay rates (k_{EET}, k_{don}, and k_{acc}) and by assuming that the initial populations ($N^{(1)}_{donor}(0)$ and $N_{acc}(0)$) are proportional to the number of each type of chromophore present in the molecule and their measured absorption coefficients at the excitation wavelength, 400 nm. Note that if $N_{acc}(0) \ll N^{(1)}_{donor}(0)$, then the amplitudes of the two components are essentially equal. In the case of the G3 dendrimer, for example, we obtain k_{EET} in the usual manner from τ_1, the fast component of the donor decay

$$k_{EET} = \frac{1}{\tau_{EET}} = \frac{1}{\tau_1} - \frac{1}{\tau_{donor}} \qquad (6)$$

Since there are 16 donors and a single acceptor in G3, and the relative ratios of the absorption coefficients are known, we have

$$N^{(1)}_{donor}(0) \propto 0.9 \times 16 \times \epsilon_{donor}(400\ nm)$$

$$N_{acc}(0) \propto 1 \times \epsilon_{acc}(400\ nm)$$

where we have taken into account that in G3 10% of the donors do not participate in the EET. Using the values $\epsilon_{donor}(400\ nm) = 11800$ and $\epsilon_{acc}(400\ nm) = 5500$, we find that the relative amplitudes of rise and decay terms should be equal to within a few percent. If we fix the acceptor and donor decay rates to be those in Tables 1 and 4, and then allow the amplitudes of the multiexponential fit to vary, then we do find that the amplitude of the rising component and the sum of the two decaying components are the same to within 5%. Figure 6b shows the signal calculated using the parameters discussed above, along with the times and amplitudes listed in Table 2, overlaid with the experimental signal. As can be seen from the figure, the agreement between the two is reasonably good. Similar calculations can be done for G0−G2, but are complicated by the more rapid EET rate, which means that the time-response of the detection system must be taken explicitly into account. This complicates the fitting, although preliminary data workup shows that the expected trends are present in the other data sets as well. In any case, the results shown in Figure 6 demonstrate that our model reproduces not only the rapid EET seen in the donor fluorescence, but also the evolution of the acceptor fluorescence.

Using the parameters extracted from our time-resolved data, we can make a separate estimation of the EET efficiencies using the relation

$$\eta_{EET} = \frac{k_{EET}}{k_{EET} + k_{donor}} = \frac{k^{(obs)}_{Fl} - k_{donor}}{k^{(obs)}_{Fl}} \qquad (7)$$

We obtain efficiencies of 0.97, 0.95, 0.91, and 0.89 for G0−G3, respectively. These efficiencies are consistently about 10% higher than those obtained from the steady-state data. The origin of this discrepancy probably lies in our assumption that the only contributions to the donor decay are energy transfer k_{EET} and its intrinsic lifetime k_{donor} which is measured using compound **6**. In reality, there can be other nonradiative channels in the dendrimers (donor aggregation, conformational distortion, and rapid electron transfer) which quench the donor fluorescence without leaving an excited acceptor. The steady-state calculations automatically take such processes into account, while our simple kinetic model neglects them and lead to an overestimation of the EET efficiencies.[12c,18] In light of the high efficiencies calculated using both the steady-state and time-resolved data, these channels are relatively minor in the compounds studied here, and our neglect of them in the modeling does not affect the main conclusions of this paper.

Unlike the nanosecond decay time, the short-time decay of the donor luminescence shows a marked dependence on dendrimer size. The Forster radius R_0 for the pyrene−benzthiadiazole donor−acceptor pair is 48 Angstroms in toluene, and all the dendrimers are smaller than this length, so the rapid EET times are consistent with a Forster mechanism. In Figure 7 we plot τ_{EET}, obtained using eq 6, as a function of dendrimer generation. Although the fluorescence lifetimes of the donor differ between solvents, we expect that the R_0 values will also change because of a solvent dependent fluorescence quantum yield, and therefore the t_{EET} curves will be similar for the different solvents. Although we only show the values obtained for the dendrimers in DMF, very similar curves are obtained

Table 2. Fit Parameters for Curve Shown in Figure 6b[a]

	A	τ (ps)
component 1	-1.603	162.2
component 2	1.157	900
component 3	0.385	2490

[a] The τ times, which are obtained from the decays of **4** and **5**, are not allowed to vary.

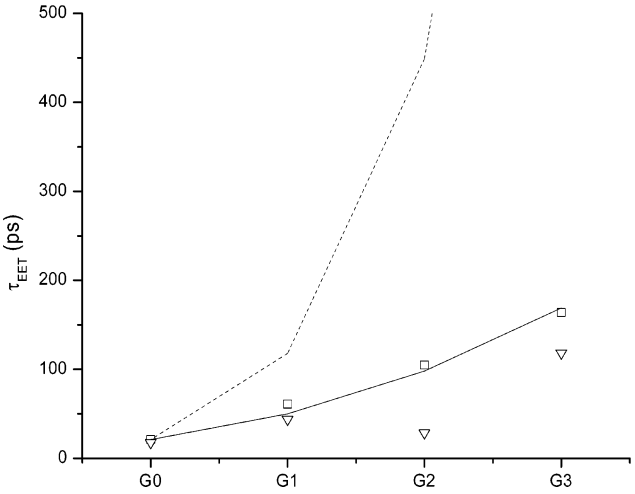

Figure 7. Measured electronic energy transfer times (τ_{EET}) are shown as squares. The triangles are the electronic energy transfer times calculated from the sum of the energy transfer rates using the donor−acceptor distances, R, from MM2 minimizations. The N^6 (dashed) and N^3 (solid) lines are shown normalized to the G0 value, where N is the number of bonds between the donor and acceptor for each molecule. Distance values are shown in Table 3.

(18) Mugnier, J.; Pouget, J.; Bourson, J.; Valeur, B. *J. Lumin.* **1985**, *33*, 273.

for toluene and CH_2Cl_2. If the EET is due to a Förster process, we expect τ_{EET} to scale as R^6, where R is the center-to-center distance between the donor and acceptor. The question then arises as to how R changes as the size of the dendrimer increases. One approach is to simply assume that R is directly proportional to the number of intervening bonds. This basically assumes a fully extended structure of the dendrimer, as shown in Chart 1, where the overall molecular size increases linearly with N, the number of bonds between donor and acceptor. In this case, $\tau_{EET} \propto R^6 \propto N$,[6] which allows us to calculate how τ_{EET} should scale with dendrimer generation. The results of such a calculation are shown in Figure 7, where the calculated rates have been scaled to match the measured G0 value. This simple estimation of the energy transfer rate clearly overestimates the sensitivity of τ_{EET} to dendrimer size. This is not surprising, since the benzyl-ether linkages are known to be quite flexible. A more realistic model would take the flexibility of the dendrimer arms into account. In the case of a flexible polymer, the actual extent of the chain increases as $\sqrt{N}$, rather than N.[19] If we naively assume that the same physics applies to the benzyl-ether arms of the dendrimer, we have $\tau_{EET} \propto R^6 \propto (\sqrt{N})^6 = N^3$. We see from Figure 7 that such a calculation does a much better job of reproducing the experimental results.

It is not immediately clear that a model developed for polymers can also be applied to these relatively small benzyl-ether dendrimers, so we have also used the MM2 force-field to examine the low energy conformers of G0−G3. As has been observed previously,[20] we see considerable backfolding in these molecules with multiple conformations separated by less than kT, the available thermal energy at room temperature. In Figure 7, we plot the τ_{EET} dependence on generation as estimated from the MM2 calculations, assuming isotropic transfer and $R_0 =$ 48 Angstroms. The total EET rate is taken to be the average of the rates due to each donor in the low energy structure

$$\frac{1}{\tau_{EET}} = \frac{1}{\tau_{donor}} \sum_{i=1}^{M} \frac{R_0^6}{R_i^6} \tag{8}$$

where R_i is the distance of each donor in the structure, and M ranges from 2 (G0) to 16 (G3). The average distances obtained for the calculations, along with the standard deviations, are shown in Table 3, along with the R distances obtained using the standard Förster relation

$$\tau_{EET} = \tau_{donor} \frac{R^6}{R_0^6} \tag{9}$$

with $\tau_{donor} = 4.95$ ns, the lifetime of the amino-pyrene **6** in the absence of the dendrimer. The agreement between the experimentally measured τ_{EET} and that calculated from the MM2 distances is fairly good, considering that the MM2 calculations were only a single run, which is not guaranteed to find the global minimum. The reason multiple runs were not done is that these runs are prohibitively slow for the larger dendrons.

(19) Tanford, C. *Physical Chemistry of Macromolecules*; Wiley & Sons: New York, 1961.
(20) For example of studies suggesting backfolding, see: (a) Wooley, K. L.; Klug, C. A.; Tasaki, K.; Schaefer, J. *J. Am. Chem. Soc.* **1997**, *119*, 53. (b) Gorman, C. B.; Hager, M. W.; Parkhurst, B. L.; Smith, J. C. *Macromolecules* **1998**, *31*, 815.

Table 3. Distances for EET Calculations from N, $\sqrt{N}$, and MM2 Calculations, along with the Experimental τ_{EET} Values and the Distances Computed from them

	τ_{EET} (ps) from eq 6	experimental R (Å) calculated using eq 8	average D–A distance and standard deviation in Å from MM2 calculations	N	$\sqrt{N}$
G0	21.2	19.3	18.8 ± 0.6	15	3.87
G1	61.7	23.1	22.6 ± 2.6	20	4.47
G2	106	25.3	24.7 ± 4.9	25	5
G3	167	27.2	28.9 ± 4.8	30	5.48

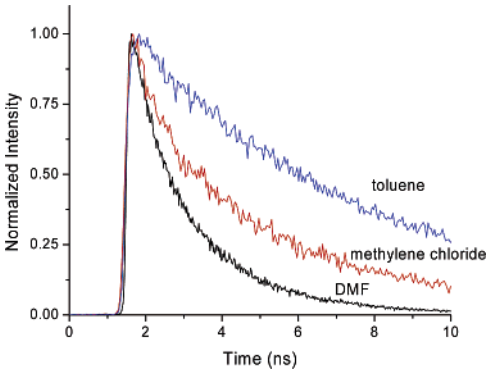

Figure 8. Acceptor emission of G2 dendrimer **3** shown in toluene (blue), methylene chloride (red), and DMF (black).

Our results in these dendrimers are consistent with flexible, backfolded arms that enable very rapid EET even in the largest dendrimer, G3. The flexibility of the benzyl-ether linkages means that τ_{EET} only scales as the square root of dendrimer size, rather than linearly as would be expected in a rigid structure. The fact that each donor also includes a tri-arylamine (TAA) group containing pyrene led us to investigate whether charge transfer could also be observed in these molecules. Electron transfer from the TAA group to the excited benzthiadiazole is expected to quench the core fluorescence at 600 nm. Furthermore, this quenching should become more pronounced in polar solvents, which increase the CT rate. Indeed, this is what is seen in Figure 8, where the acceptor decay for the G2 dendrimer becomes more rapid as we go from nonpolar solvents (toluene) to very polar solvents (DMF). This trend of more rapid fluorescence decays in more polar solvents is the same for the other dendrimers as well. In general, the fluorescence decays are slightly nonexponential, and in some cases were fit using biexponentials. The results of our fits to the acceptor fluorescence decays in toluene, CH_2Cl_2, and DMF for dendrimers G0-G3 are given in Table 4. From the data in Table 4, we estimate the CT efficiency using the relation

$$\eta_{CT} = \frac{k_{CT}}{k_{acc}} = \frac{k_{acc} - k_{acc}^0}{k_{acc}} \tag{10}$$

where k_{acc}^0 is the fluorescence decay rate of the acceptor without the attached dendrimer, and where k_{acc}, in the case of a biexponential decay is given by

$$k_{acc} = \frac{A + B}{A\tau_A + B\tau_B} \tag{11}$$

Using these relations and the values in Table 4, for example,

Table 4. Acceptor Fluorescence Decays (excited at 400 nm) and CT Efficiencies Calculated Using eq 10[a]

	toluene					methylene chloride					DMF				
	A	τ_A	B	τ_B	η_{CT}	A	τ_A	B	τ_B	η_{CT}	A	τ_A	B	τ_B	η_{CT}
acceptor		6.62					7.66					7.49			
G0		6.59			0.0045		4.97			0.351		1.72			0.770
G1		6.51			0.0166	0.64	5.36	0.36	1.95	0.461	0.76	2.57	0.24	1.17	0.702
G2	0.95	6.56	0.05	0.44	0.0553	0.62	4.76	0.38	0.98	0.566	0.51	2.24	0.49	0.89	0.789
G3	0.93	6.98	0.07	1.43	0.0042	0.60	5.49	0.40	1.00	0.518	0.37	2.49	0.63	0.90	0.805

[a] Decays with two time scales are fit with a biexponential fit of the form $A \exp[(-t/\tau_A)] + B \exp[(-t/\tau_B)]$. All times are in ns.

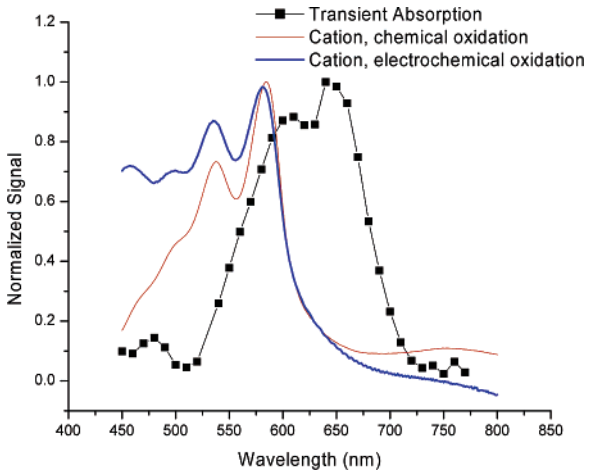

Figure 9. Absorption spectrum of the amino-pyrene compound **6** after oxidation using a stoichiometric amount of $SbCl_5$ (red), after electrochemical oxidation (blue) and transient absorption of G3 in DMF (squares).

we calculate that G0 in DMF has a 77% yield of charge separated species, based on the fluorescence quenching alone.

The presence of a charge separated state can be confirmed using transient absorption on the microsecond time scale, after the initial singlet excited-state emissions and absorptions have decayed. We have done nanosecond experiments on the dendrimers in the same solvents in which we did the fluorescence measurements. For the acceptor by itself in any solvent, and for the dendrimers in nonpolar toluene, no long-lived (>10 ns) transient absorption could be detected, as expected in the absence of charge transfer. But in both CH_2Cl_2 and DMF, very similar induced absorptions in the visible region were observed. Figure 9 shows this absorption in G3, along with the absorption measured when compound **6** is oxidized, either using $SbCl_5$ or electrochemically. A similar absorption is observed for dendrimers G1 and G2 as well, although our signal-to-noise was not sufficient to resolve this feature in G0. The absorption spectra of radical cation of the TAA and of the long-lived species produced by photoexcitation of the dendrimers are similar in shape, but the dendrimer transient absorption is redshifted by about 50 nm. Such a redshift can be due to either solvatochromic effects within the polarizable dendrimer environment or the radical anion of benzthiadiazole as the counterion, which are not present in the model compound. In both cases, one could expect the observed red shift. The lifetime of this species depends on solvent polarity. In DMF, the lifetime of the absorption decays varies from 2 to 3 μs and shows no systematic trend with dendrimer size. In CH_2Cl_2, the lifetime ranges from 0.9 to 1.6 μs for all dendrimers, as expected if the stability of the charge separated state is decreased in this less polar solvent. In light of the similarity of the transient absorption spectrum with that obtained using chemical and electrochemical oxidation methods, its long lifetime and its behavior with solvent polarity, we can assign the induced absorption to the radical cation of the TAA donor group.

The photophysics indicate that after EET from the peripheral donors to the core acceptor, an electron is then transferred from one of the donors to the excited core. Due to experimental limitations, we were unable to independently obtain a quantum yield for the generation of the CT species from the transient absorption experiments, and so we must rely on the fluorescence quenching to estimate the CT quantum yield. We note that these efficiencies represent an upper bound on the actual yield, since they do not take into account the possible contributions of other nonradiative processes (intersystem crossing, internal conversion) which might also be solvent dependent. There is no experimental evidence that such processes play a significant role in the current experiments, e.g., no large triplet absorption was observed in the transient absorption experiments. Also, we have synthesized dendrimers with benzyl ether arms without the diarylaminopyrene donors incorporated in them. The fluorescence lifetime of the core benzthiadiazole is unaffected by the presence of various generations of benzyl ether dendrons. The lifetimes range from 6 ns in toluene to 7 ns in CH_2Cl_2 to 8 ns in DMF. In other words, there is no evidence that the addition of benzyl ether backbone leads to an increase in other nonradiative processes. The yields obtained from the fluorescence quenching are reasonably high, and if we multiply the yield for energy transfer in G3 (0.81) by the yield for CT (0.70), we obtain an overall efficiency, absorption to charge separated state, on the order of 50%. This efficiency is probably limited by the fact that CT must occur within the nanosecond singlet lifetime of the core benzthiadiazole. If the core could rapidly cross to a long-lived triplet with favorable redox properties, like C_{60}, then we would anticipate a significant increase in the CT yield.

Perhaps more interesting is the fact that the CT yield does not appear to have any significant dependence on dendrimer size, as can be seen from Table 4. This is especially surprising in light of the fact that τ_{EET} exhibited a strong generation dependence as seen in Figure 7. The most likely explanation for this lack of size dependence in the CT rate is that the overall CT rate only depends on the distance of the closest ground state electron donor. The backfolding observed in these systems provides many opportunities for the TAA groups to closely approach the core. In the case of EET, the incoming photon excites all donors with equal probability, so even if one is close, the overall rate will reflect the contribution from the more distant donors as well. But the CT event will only reflect the presence of the nearest donor, and if that distance of closest approach is roughly equal in all the dendrimers, then the net CT rate will also be the same. As the dendrimer size increases, the average distance to the peripheral donors increases, but the additional

donors also provide more opportunities for conformational disorder to bring one back into contact with the core. Such an increase in disorder with increasing size can be seen from the standard deviation data in Table 3. If this hypothesis is correct, then the key to maintaining reasonable CT rates with larger dendrimers is to maintain the flexibility of the backbone.

Other CT mechanisms such as the more classical through-bond tunneling or solvent assisted mechanisms are possible. If the CT event is based on a through-bond mechanism, then a systematic dependence (or generation dependence) would be expected. However, this trend is complicated by the fact that the number of TAA units increase with generation, which will have the opposing effect on the CT quenching efficiency. It is also possible that the conformational changes by the solvent has an effect on CT. If this were the case in these dendrimers, then significant differences in EET efficiencies should have been observed in different solvents. Therefore, we believe that this mechanism is less likely. We believe that the observations could be more simply explained by the mechanism proposed in the previous paragraph. Experiments that could clearly distinguish these mechanistic possibilities are also underway in our laboratories.

Experimental Section

All experimental details are provided as Supporting Information to this paper.

Conclusion

We have studied the photophysical properties of a family of benzyl-ether based dendrimers, which exhibit both light-harvesting and electron-transfer functionalities. The large (80−90%) energy transfer efficiencies scale favorably with increasing dendrimer size. The reason τ_{EET} is observed to scale only as $\sqrt{N}$, as opposed to the N scaling expected in a rigid structure, is the ability of the flexible arms to backfold and decrease the average distance between donor and acceptor. As observed previously by Frechet and co-workers,[21] this flexibility apparently does not come at the cost of increasing donor aggregation and decreased energy transfer efficiency. After energy transfer, these molecules show fluorescence quenching and transient absorption characteristic of the creation of long-lived charge-transfer states. Estimates based on fluorescence quenching indicate CT efficiencies as high as 70% in the most polar solvent, DMF. Although these yields may be taken as upper limits, the present work clearly demonstrates that these non-conjugated, flexible dendrimers can simultaneously exhibit reasonably high energy transfer and electron transfer efficiencies which scale favorably with size.

The main goal of future work will be to investigate how to increase energy and charge transfer efficiencies. The energy transfer efficiency is currently limited by the size of the slowly decaying donor component, and identifying its origin is the key to raising the light-harvesting efficiency to close to 100%. To increase the charge transfer efficiency, one possibility we are currently pursuing is the incorporation of additional amino groups in the dendrimer arms to increase the probability of contact with the core.[22] Another area of interest is increasing the lifetime of the charge separated state. A final question which we have not addressed is the role of dynamic conformational fluctuations in enhancing energy or charge transfer processes. The flexibility of the nonconjugated dendrimer arms not only allows for more efficient packing, but may also provide transient opportunities for the approach of the electron donating amino groups to the core, facilitating charge transfer via a diffusional encounter mechanism. All of these issues suggest that multi-functional, nonconjugated dendrimers merit further study.

Acknowledgment. This work is supported by U.S. Department of Energy, Basic Energy Sciences program. DOE Grant (DE-FG02-04ER15503 to S.T.; DEFG02-01ER15270 to C.J.B.). We thank A. Nantalaksakul (UMass) and Dr. Gordon Hug (Radiation Lab, University of Notre Dame) for help with the transient absorption measurements. The Radiation Laboratory of the University of Notre Dame is also supported by the U.S. Department of Energy, Basic Energy Sciences program. S.T. is a Cottrell Scholar, C.J.B. is a Sloan Fellow, and A.L.T. is a NSF Predoctoral Fellow.

Supporting Information Available: All experimental details are provided in the Supporting Information. This material is available free of charge via the Internet at http://pubs.acs.org.

JA044778M

(21) Serin, J. M.; Brousmiche, D. W.; Frechet, J. M. J. *Chem. Commun.* **2002**, 2605.

(22) (a) Bronk, K.; Thayumanavan, S. *Org. Lett.* **2001**, *3*, 2057. (b) Bronk, K.; Thayumanavan, S. *J. Org. Chem.* **2003**, *68* , 5559.